NeuroImage: Clinical 31 (2021) 102698

Contents lists available at ScienceDirect

NeuroImage: Clinical

journal homepage: www.elsevier.com/locate/ynicl

Grey and white matter network disruption is associated with sensory deficits after stroke

Simon S. Kessner [1,*], Eckhard Schlemm [1,*], Christian Gerloff, Götz Thomalla, Bastian Cheng

Department of Neurology, University Medical Center Hamburg-Eppendorf, Hamburg, Germany

ARTICLE INFO

Keywords:
Sensory stroke deficit
Stroke network
Stroke lesion
Sensory recovery
Grey matter disruption
White matter disruption

ABSTRACT

Somatosensory deficits after ischaemic stroke are common and can occur in patients with lesions in the anterior parietal cortex and subcortical nuclei. It is less clear to what extent damage to white matter tracts within the somatosensory system may contribute to somatosensory deficits after stroke. We compared the roles of cortical damage and disruption of subcortical white matter tracts as correlates of somatosensory deficit after ischaemic stroke.

Clinical and imaging data were assessed in incident stroke patients. Somatosensory deficits were measured using a standardized somatosensory test. Remote effects were quantified by projecting the MRI-based segmented stroke lesions onto a predefined atlas of white matter connectivity. Direct ischaemic damage to grey matter was computed by lesion overlap with grey matter areas. The association between lesion impact scores and sensory deficit was assessed statistically.

In 101 patients, median sensory score was 188/193 (97.4%). Lesion volume was associated with somatosensory deficit, explaining 23.3% of variance. Beyond this, the stroke-induced grey and white matter disruption within a subnetwork of the postcentral, supramarginal, and transverse temporal gyri explained an additional 14% of the somatosensory outcome variability. On mutual comparison, white matter network disruption was a stronger predictor than grey matter damage.

Ischaemic damage to both grey and white matter are structural correlates of acute somatosensory disturbance after ischaemic stroke. Our data suggest that white matter integrity of a somatosensory network of primary and secondary cortex is a prerequisite for normal processing of somatosensory inputs and might be considered as an additional parameter for stroke outcome prediction in the future.

1. Introduction

Somatosensory deficits are common, occurring in about sixty percent of stroke survivors (Kessner et al., 2016; Sullivan and Hedman, 2008). Since impaired sensation affects long-term functional outcome, it is important to understand how brain damage induced by stroke shapes somatosensory deficits (Patel et al., 2000). Somatosensory input enters the brainstem and projects to the cerebellum and the thalamus. Postsynaptic processing includes the primary (SI) and secondary (SII) somatosensory cortex (Creutzfeldt, 1983; Zilles and Rehkämper, 1993). The primary somatosensory cortex is parcellated into 4 Brodman areas (BA 1, BA 2, BA 3a, BA 3b) with distinct roles (Brodman, 1909). The parietal operculum and more specifically OP1, which is a major area of the human SII, plays an important role in sensory processing in human studies (Eickhoff et al., 2006b; 2006a;; Grefkes and Fink, 2007). Beyond SI and SII, sensory inputs are further processed and integrated in associative cortex areas, sometimes mentioned as tertiary somatosensory cortex. Depending on the site of a lesion, distinct sensory syndromes are described (Klingner et al., 2012). Damage to the brainstem may cause dissociated loss or dysfunction of pain and temperature sensation (lateral) or vibration and position sense (medial); thalamic lesions may present with numbness and paraesthesia in association with pain; the cortical sensory syndrome, which can result from parietal cortical stroke, comprises discriminative impairments in stereognosis, proprioception, or texture discrimination.

Larger infarct volumes are associated with greater somatosensory deficits (Hawe et al., 2018). However, lesion size only partly determines the clinical severity of ischaemic stroke (Page et al., 2013). Additional

* Corresponding authors at: University Medical Center Hamburg-Eppendorf, Department of Neurology, Martinistr. 52, D-20246 Hamburg, Germany.
E-mail addresses: s.kessner@uke.de (S.S. Kessner), e.schlemm@uke.de (E. Schlemm).
[1] These authors contributed equally to this work.

https://doi.org/10.1016/j.nicl.2021.102698
Received 7 November 2020; Received in revised form 7 May 2021; Accepted 8 May 2021
Available online 11 May 2021

information is contained in the anatomical location of the lesion and its consequent disruption of cortical areas associated with specific neurological functions or white matter tracts that allow for distributed processing of brain functions (Wu et al., 2015).

A purely geometric analysis often aims to associate the clinical outcome of interest with the presence or absence of ischaemic damage in predefined anatomical regions ranging in size from individual voxels (Meyer et al., 2016) to territories of cerebral arteries (Rothwell, 2002). Imaging studies have implicated damage to the primary and secondary sensory areas, the insular cortex and the brainstem, thalamus, internal capsule, and corona radiata to be relevant for somatosensory deficits after stroke (Kim, 1992; Shintani et al., 1994). Voxel-based lesion symptom mapping studies (Rorden et al., 2007) in stroke patients have linked the posterior insula with impaired temperature perception (Baier et al., 2014), while deficits in proprioception were associated with lesions in sensorimotor, superior temporal, supramarginal, insular, and opercular cortex (Kenzie et al., 2016). Impaired light touch sensation may result from stroke lesions in the parietal operculum, the insula, the putamen, and frontal subcortical pathways (Preusser et al., 2014).

While these approaches focus on localized associations between brain structure and behaviour, lesion network studies capitalise on knowledge about connectivity between brain areas to study remote effects of a lesion and how it disrupts the global organisation of the brain network (Boes et al., 2015; Gleichgerrcht et al., 2017; Griffis et al., 2019; Kuceyeski et al., 2016). Lesion-network studies of the structural connectome have broadened our understanding of neuroanatomical correlates of post-stroke deficits in motor function (Cheng et al., 2019; Schlemm et al., 2020), speech (Gleichgerrcht et al., 2015), and spatial perception (Vaessen et al., 2016). However, investigations of lesion impact on large-scale structural connectivity underlying somatosensory impairments are lacking.

We therefore investigated the impact of stroke lesions on the structural connectome in relation to somatosensory deficits (Kessner et al., 2019). We analysed clinical and imaging data from the recent TOpological and clinical PrOspective study about Somatosensation in Stroke (TOPOS). After projecting stroke lesions onto white and grey matter atlases we extracted spatially and topologically specific lesion impact scores that were assessed for association with clinical parameters. We hypothesized that sensory deficits would relate to grey and white matter integrity in somatosensory networks and that network disruption would explain additional variation in clinical outcome beyond lesion volume.

2. Methods

2.1. Patient recruitment

For this analysis, clinical and imaging data from the TOPOS study were used. TOPOS was a prospective observational study that included consecutive patients with incident stroke who were admitted to the Stroke Unit of the Department of Neurology of the University Medical Centre Hamburg-Eppendorf in Hamburg, Germany, between 2014 and 2017 (Kessner et al., 2019). The local ethics committee (Ethikkommission der Ärztekammer Hamburg) approved the study prior to enrolment. Inclusion criteria were age over 18 years, first-ever ischaemic stroke with acute brain lesion observed in MRI or CT, feasible clinical examination within four days after onset, and written informed consent. Exclusion criteria were transitory ischaemic attack, spinal infarction, severe aphasia, neglect or severe cognitive deficit or reduced consciousness, or any previous condition with substantial involvement of the nervous system such as head trauma, intracranial malignant neoplasms or polyneuropathy. Radiological evidence of cerebral small vessel disease was not considered an exclusion criterion.

2.2. Clinical evaluation

Somatosensory deficits in the acute phase 3–5 days after stroke were measured using the Rivermead Assessment of Somatosensory Performance (RASP) battery (Winward et al., 2002), which consists of standardized tests for perceptive deficits of the following somatosensory modalities: pressure touch, hot–cold-discrimination, sharp-dull-discrimination, bilateral touch discrimination, joint movement, and passive movement direction discrimination. In addition, we assessed light touch perception on the cheeks, the shoulders, the palms of the hand, on the legs, and on the dorsum of the feet using a cotton swab. During administration of the RASP, sham trials were performed to reduce bias due to guessing. Each correct recognition of an applied stimulus increases the counts and thus higher scores represent better performance. Taken together, the possible maximum score of the RASP per body side is 193 points.

Additionally, in order to characterise the study population and inform translation of our result to other cohorts, demographic and basic clinical assessments were collected such as the National Institutes of Health Stroke Scale (NIHSS) score, and the Barthel index.

2.3. Image acquisition and processing

Magnetic resonance imaging (MRI) of the brain was performed in the acute phase 3–5 days after stroke. Using 1.5 and 3.0 Tesla MRI scanners, anatomical (T1), fluid-attenuated inversion recovery (FLAIR) and diffusion-weighted (DWI) sequences were acquired using the following sequence parameters: T1 (1.5 T): repetition time 9.3 ms, echo time 4.76 ms, pixel spacing 0.5x0.5 mm^2, acquisition matrix 256x192, field of view 256x192mm^2, slice thickness 1 mm, number of slices 160. FLAIR (1.5 T): repetition time 8000 ms, echo time 103 ms, inversion time 2370 ms, pixel spacing 0.449x0.449 mm^2, acquisition matrix 256x144, field of view 230x172mm^2, slice thickness 5 mm, number of slices 26, spacing between slices 6.5 mm. DWI (1.5 T): repetition time 4000 ms, echo time 84 ms, pixel spacing 1.875x1.875 mm^2, acquisition matrix 128x128, field of view 240x240mm^2, slice thickness 4 mm, number of slices 30, spacing between slices 4 mm, b-value 1000. T1 (3 T): repetition time 8.13 ms, echo time 3.72 ms, pixel spacing 0.9375x0.9375 mm^2, acquisition matrix 240x155, slice thickness 1 mm, number of slices 160, spacing between slices 1 mm. FLAIR (3 T): repetition time 4800 ms, echo time 376.475 ms, inversion time 1650 ms, pixel spacing 0.744x0.744 mm^2, acquisition matrix 332x332, slice thickness 3 mm, number of slices 55, spacing between slices 3 mm. DWI (3 T): repetition time 2796 ms, echo time 86 ms, pixel spacing 1.03x1.03 mm^2, acquisition matrix 152x106, slice thickness 5 mm, number of slices 22, spacing between slices 6 mm, b-value 1000.

Semi-automated stroke lesion segmentation was performed based on the FLAIR image using an in-house software ANTONIA, as described previously (Forkert et al., 2014). In two cases, computed tomography scans were performed instead due to contraindications to MRI. Here, infarcts were segmented with FSL software package 5.1. by manual delineation. Native FLAIR / T1 weighted images were registered to standard Montreal Neurological Institute (MNI) space using linear registration algorithm FLIRT with 6 degrees of freedom. Linear preprocessing was chosen because non-linear native brain image registration to the MNI template is challenging in images with large brain infarct lesions, particularly at the acute period. If necessary for transformation accuracy, the pathological region (lesion) was masked out during coregistration process. Transformation matrices were extracted and used to map the binary lesion masks into MNI space, where they were mirrored to the right hemisphere.

2.4. Quantification of network disruption

The structural brain connectome is an abstract representation of the interconnections between different grey and white matter areas that form the macro-anatomical substrate for the spatial and temporal coordination of distributed neuronal function. It can be described as a network, consisting of a finite set of nodes and edges between them, that represent grey matter

areas and white matter fibre tracts, respectively (Sporns, 2013). A focal lesion can disrupt the network architecture by affecting either one or both of these components (Griffis et al., 2019). We applied two distinct methodologies to evaluate the effect of stroke lesions on nodes and edges of the structural connectome as illustrated in Fig. 1.

First, in order to quantify the effect of stroke lesions on structural connectivity, binary masks in MNI space were entered into the Network Modification (NeMo) Toolbox for Matlab and projected onto a set of 73 structural reference tractograms obtained from healthy participants (Kuceyeski et al., 2013). Based on the Desikan-Killiany atlas (Desikan et al., 2006) a parcellation of the stroke hemisphere into 42 prespecified regions, including seven subcortical areas, was defined (Supplementary Tab. 1). For each of those regions and each subject, the proportion of incident diffusion streamlines running through that subject's stroke lesion mask was computed. This proportion, termed Change in Connectivity (ChaCo) score, quantifies disruption in the fibre tracts related to each grey matter region of the parcellation. It ranges from zero (no disruption) to a maximum value of 1 (complete disconnection of a region from the rest of the network). Importantly, the so-computed ChaCo score reflects both disturbed short-range connectivity within a brain region, as mediated for instance by cortical U fibres, and long-range connectivity between different brain regions. This structural lesion network mapping approach thus associates white matter damage at different locations with disturbed connectivity of grey matter regions in a topologically specific way. In contrast to the brain-wide disruption of connectivity induced by a stroke lesion, we therefore refer to a region's ChaCo score also as its local disconnection. In order to focus on the relative importance of white and grey matter network disruption at the aggregate level of brain regions, pairwise disconnectivity was not estimated for this analysis. The validity of the Network Modification approach has previously been established in applications to localise brain circuits underlying activities of daily living and cognition (Kuceyeski et al., 2015) and to predict tissue loss and functional outcome after stroke (Griffis et al., 2019; Kuceyeski et al., 2014).

Second, disruption of connectome nodes was evaluated by calculating, for each stroke lesion, the overlap with individual, prespecified grey matter regions defined by the same modified Desikan-Killiany atlas. After division by the region volume, this process resulted, for each subject, in 42 normalised Node Destruction (*NoDe*) scores, ranging from zero for regions not affected by a stroke lesion to one for grey matter regions entirely contained within a stroke lesion. By definition, white-matter components of stroke lesions did not contribute to NoDe scores.

2.5. Statistical analysis

The clinical outcome variable RASP was transformed into a somatosensory deficit (SSD) score by subtracting individual values from the theoretical maximum of 193. Scores were then summarised by median and interquartile range. The association between infarct volume and clinical deficit in the acute phase was quantified using generalised linear regression models with a logarithmic link function and quasi-Poisson response distribution.

Direct ischaemic damage and loss of connectivity in each of 42 brain regions of the modified Desikan-Killiany parcellation was summarised by median and interquartile range of NoDe and ChaCo scores, respectively. Both region-specific markers of network disruptions were assessed for association with somatosensory deficits using mass-univariate generalised linear regression analyses as above. Regression coefficients with 95% confidence intervals, as well as the Akaike information criterion (AIC) as an estimate of out-of-sample prediction error were calculated for each brain region and either type of network disturbance. Type-I error inflation was controlled using the Bonferroni-Holm method (Sture Holm, 1979).

Given the fact that stroke lesions are rarely purely cortical and usually extend into the underlying white matter, we expected a high degree of statistical dependence between ChaCo (edge disruption) and NoDe (node disruption) scores, especially when restricted to lesions with cortical involvement. In order to further assess the relative importance of grey matter and white matter disruptions on somatosensory pro-

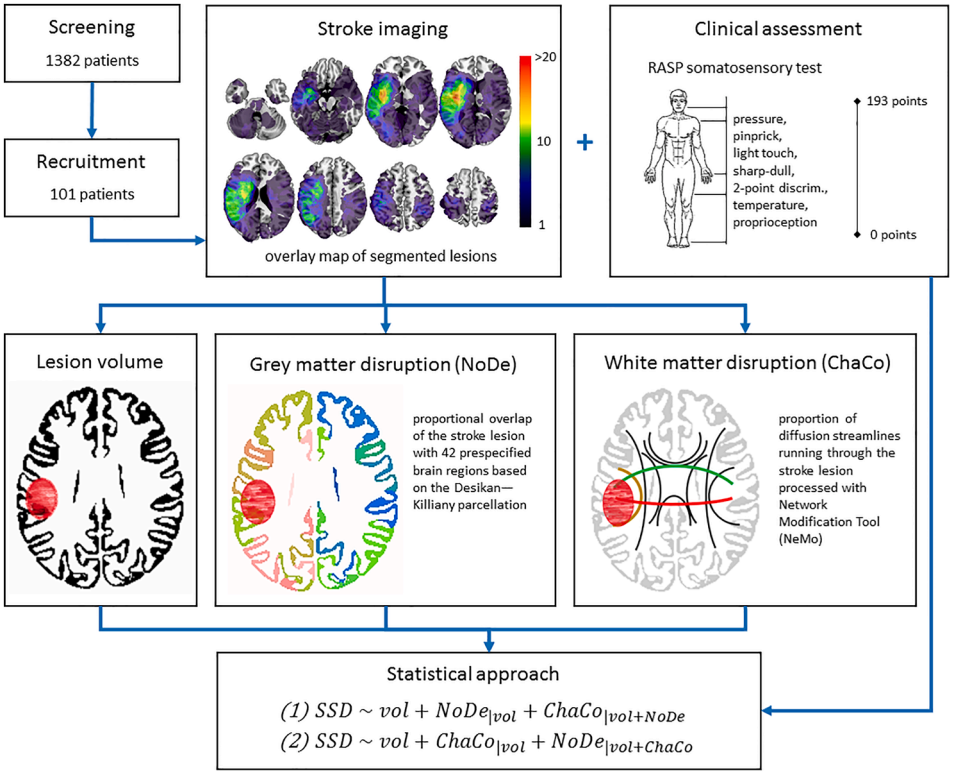

Fig. 1. Methodological flowchart for the study. After screening, all recruited patients underwent acute MR or CT brain imaging for stroke lesion segmentation. In the acute phase, after 3, and after 12 months, patients were clinically assessed for somatosensory deficits using the Rivermead Assessment for Somatosensory Performance (RASP). Lesion images were assessed for volume. Direct involvement of prespecified regions was calculated based on lesion overlap as a surrogate marker for grey matter node destruction (NoDe). White matter disruption was computed using the Network Modification Toolbox (NeMo) resulting in region-specific change of connectivity score (ChaCo). The three imaging parameters volume, NoDe and ChaCo were subsequently entered into statistical models and assessed for association with acute somatosensory deficit (SSD).

cessing in the context of this collinearity, we computed semi-partial correlations, corrected for lesion volume, of both ChaCo and NoDe scores with sensory deficit scores. More precisely, we fitted models of the form

$$SSD \sim vol + NoDe_{|vol} + ChaCo_{|vol+NoDe} \quad (1)$$

$$SSD \sim vol + ChaCo_{|vol} + NoDe_{|vol+ChaCo} \quad (2)$$

where SSD represents somatosensory deficit scores as defined above, and the subscripted vertical bar denotes linear residualisation. We quantified the unique contribution of grey and white matter disruption to explaining variation in the clinical outcome as the incremental deviance attributable to the right-most predictors in models (1) and (2). The statistical significance of these contributions was assessed using likelihood-ratio tests. We use the term predictor to refer to independent variables in a regression model; no attempt is made, in this work, to forecast long-term outcomes from acute imaging parameters. Statistical analyses were performed in the R Statistical Computing Environment (R Development Core Team 3.0.1., 2013).

3. Results

3.1. Patient demographics and clinical data

Based on a total of 1382 screened patients, 101 patients were included in this study and completed the acute assessment including brain imaging and clinical testing. Demographics and clinical outcomes are given in Table 1; for recruitment details see Supplemental Fig. S4 and the previously published sample description (Kessner et al., 2019). The majority of lesions (n = 82, 81%) were distributed across the forebrain, seven of which exclusively impacted the cortex, while 34 were located purely subcortically, affecting white matter and/or subcortical nuclei such as the basal ganglia and the thalamus, and 41 lesions involved both cortical and subcortical compartments. The remaining 19 lesions were situated in the brainstem or cerebellum. Clinically, in the acute phase after stroke onset, RASP scores ranged from 3 to 193 points with a median of 188 points (interquartile range 160–192). A detailed behavioural and longitudinal analysis has been reported previously (Kessner et al., 2019).

3.2. Effect of lesion volume

Stroke lesion volume on acute brain imaging ranged from 0.01 ml to 232 ml (median 6 ml, IQR 1–30 ml). In generalised linear regression modelling, every 10-fold increase in size of the infarct on initial imaging was associated with a 2.29-fold ($CI_{95\%}$ [1.64, 3.29]) increase in somatosensory deficits (P 0.948e-06), see Fig. 2. The proportion of deviance explained by the model was 23.30%. This association persisted essentially unchanged after removing four potentially influential observations as identified by large values of Cook's distance measure, studentized residuals or leverage (Fox et al., 2011), with an estimated effect size of 2.24 ($CI_{95\%}$ [1.57, 3.29], P 0.410e-06) and 20.9% explained deviance. More detailed statistical diagnostics and clinical data relating to these influential observations are provided in the Supplement (Figs. S1, S2).

3.3. Network disruption

Extent of disruption of structural connectivity and damage to cortical und subcortical grey matter areas induced by stroke lesions are illustrated in Fig. 3. Findings are based on the pre-specified augmented Desikan-Killiany parcellation scheme with 35 cortical and 7 subcortical areas as implemented in the NeMo toolbox (Desikan et al., 2006; Kuceyeski et al., 2013).

Network disruption with regard to edges of the structural connectome representing white matter tracts was spatially heterogeneous. Most prominent disruptions of structural connectivity (highest ChaCo scores) were observed for subcortical regions as well as cortical areas adjacent to the central sulcus (Supplementary Tab. 2). The thalamus and hypothalamus were affected by disconnection in almost all subjects (99.0%) with an average non-zero ChaCo score of 6.7% and 4.4%, respectively. Pallidum, hippocampus, caudate nucleus and putamen were affected in 93.1%, 93.1%, 92.1% and 91.1% of the patients. The proportion of streamlines in the standard connectome that had the pallidum, hippocampus, caudate nucleus or putamen as one of their

Table 1
Demographic, clinical, and stroke lesion characteristics of the 101 included patients. RASP = Rivermead Assessment of Somatosensory Performance. NIHSS = National Institutes of Health Stroke Scale.

Demographics				
Age at onset [years]	**median**	**minimum**	**maximum**	**interquartile range**
	64	29	88	54–72
Sex	**female**	**male**		
	32	69		
Highest education	**middle school**	**high school**	**vocational training**	**academic degree**
	17	1	60	23
Clinical characteristics				
	median	**mean**	**min - max**	**interquartile range**
RASP (0 – 193)	188	164	3–193	160–192
NIHSS (0 – 42)	2	3.7	0–21	1–4
Barthel (0 – 100)	85	75	10–100	50–100
Lesion characteristics				
Brain compartment (n)	**Forebrain**			**Hindbrain**
	Cortical	**Subcortical**	**Combined**	
	7	34	41	19
Lesion side (n)	**right**	**left**		
all patients	65	36		
cortical	6	1		
subcortical	21	13		
combined	28	13		
brainstem / cerebellum	11	8		
Lesion volume [ml]	**median**	**min - max**	**interquartile range**	
all patients	6	0.01–232	1–30	
cortical	7	0.2–25	3–8	
subcortical	1	0.07–136	0.4–6	
combined	35	0.01–232	17–73	
brainstem / cerebellum	1	0.2–54	0.6–2	

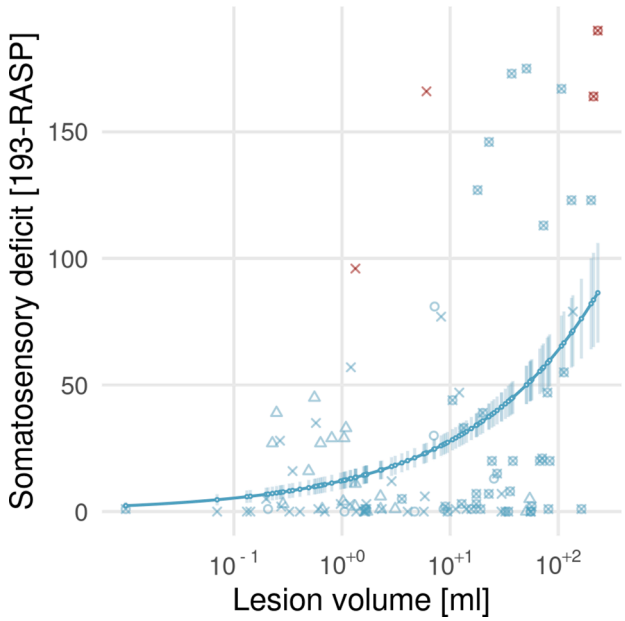

Fig. 2. Association between lesion volume and sensory deficit. Outcome is the sensory deficit (193 minus RASP score) in the acute phase 3–5 days after stroke. Markers represent individual patients with cortical (circle), subcortical (cross), combined cortico-subcortical (crossed circle), or hind brain (triangle) lesions; solid curves, conditional means in a quasi-Poisson regression model; vertical line segments, pointwise 95% confidence intervals. Four influential points, omitted in a sensitivity analysis, are marked in red. (For interpretation of the references to colour in this figure legend, the reader is referred to the web version of this article.)

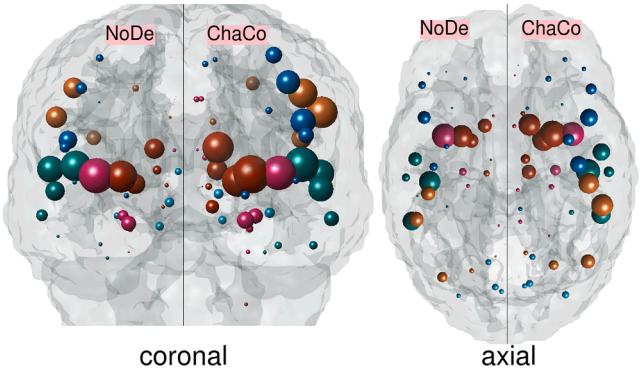

Fig. 3. Spatial distribution of structural grey and white matter network disruption. The distribution of both grey and white matter disruption in regions of the modified Desikan-Killiany parcellation induced by acute ischaemic stroke lesions in coronal and axial view. Ball volumes on the left indicate grey matter disruption defined as NoDe score (average relative overlap of a parcel with stroke lesions). Ball volumes on the right indicate white matter disruption defined as ChaCo score (average proportion of a parcel's streamlines running through a lesion). Colours indicate assignment of brain regions to frontal (●), parietal (●), temporal (●), occipital (●) and limbic (●) lobes, or subcortical structures (●).

endpoints and met, on their course, at least one voxel of the stroke lesion mask (ChaCo score), averaged across patients, was given by 11.1%, 5.2%, 10.8%, and 13.4% respectively. The most frequently disconnected cortical regions were the insular cortex (affected in 90.1% of patients, mean positive ChaCo score 12.2%); the supramarginal and precentral gyri (affected in 83.2%; mean positive ChaCo 12.1% and 9.2%); and the postcentral, superior temporal, caudal middle frontal gyri (affected in 82.2%; mean positive ChaCo score 11.5%, 9.8%, 6.5%).

Table 2 reports results of mass-univariate analyses of associations between region-specific disruption of network edges and acute sensory deficits. Controlling for the effect of lesion volume, acute impairment in sensation was significantly associated with loss of structural connectivity to and within the postcentral (beta 2.55 +/- 0.68, P_{adj} 0.013), supramarginal (beta 2.47 +/- 0.61, P_{adj} 0.005), and transverse temporal (beta = 1.73 +/- 0.49, P_{adj} 0.028) cortices. Additional numerical associations, which did not reach statistical significance after correction for multiple testing, were observed in the insula, the precentral gyrus, the inferior frontal and superior temporal cortices, as well as the posterior cingulum ($P < 0.05$, $P_{adj} < 1$).

Spatial distribution of network disruption with regard to direct damage of connectome nodes, as measured by lesion overlap with grey matter areas, was similar to dysconnectivity profiles described above (Fig. 3). Evidence of direct involvement of the grey matter in the postcentral, supramarginal and transverse temporal gyri was seen in 36.7%, 33.7% and 22.8% of patients, respectively, with, on average, 17.9%, 20.2% and 42.9% of the cortical volumes being affected by stroke lesions. The extent of cortical involvement in these areas (measured by NoDe score) was significantly associated with sensory deficits (postcentral: beta 2.18 +/- 0.65, P_{adj} 0.041; supramarginal: beta 2.27 +/- 0.59, P_{adj} 0.009; transverse temporal: beta = 1.58 +/- 0.45, P_{adj} 0.024; Table 2). In comparison to local change of connectivity, regressing sensory deficits against cortical involvement resulted in numerically larger AIC values, indicating a worse out-of-sample prediction accuracy.

In all areas, NoDe and ChaCo scores were highly correlated with each other (Supplementary Fig. 1), owing to the spatial localisation of stroke lesions involving both cortical areas and their underlying white matter tracts. In addition to the 23.3% of acute clinical outcome variation accounted for by lesion volume, the combination of grey and white matter disruption explained a significant excess proportion of clinical variation in four brain regions: supramarginal (14.4%, P_{adj} 0.007), postcentral (12.8%, P_{adj} 0.026), transverse temporal (11.7%, P_{adj} 0.048) gyri; and caudate nucleus (11.1%, P_{adj} 0.043). The unique contributions obtained from allocating outcome variation to NoDe and ChaCo scores according to the semi-partial correlation models (1) and (2) specified in the Methods section are shown in Fig. 4-B): when variation in clinical outcome was preferentially allocated to grey matter involvement (NoDe scores; upper panel), a significant amount of residual variation was accounted for by local disconnection of the supramarginal (1.9%) and postcentral (3.6%) gyrus (likelihood ratio tests applied to models (1) and (2), uncorrected $P < 0.05$). In contrast, when variation in clinical outcome was preferentially allocated to white matter damage (ChaCo scores; middle panel), no significant amount of residual variance was explained by direct damage to any brain region.

4. Discussion

Our analysis of the differential importance of grey and white matter damage as neuroanatomical correlates of disturbed somatosensory processing after ischaemic stroke yielded three main results. First, the size of the acute infarct was strongly associated with acute somatosensory deficits. Second, both geometric and topological lesion-symptom mapping localised deficits in somatosensation selectively and consistently to the same cortical areas in the anterior parietal and superior temporal lobes. Third, in a direct comparison, disruption of white matter pathways (edges, links) to the identified areas in the supramarginal and transverse temporal gyri (vertices, nodes) explained a larger proportion of variation in the acute clinical deficits than direct ischaemic damage to these areas.

In this study of 101 ischaemic stroke patients, the extent of the ischaemic lesion was strongly associated with deficits in somatosensory processing in the acute phase 3–5 days after the index event. In our population, lesion volume explained almost one quarter (23.3%) of variation in the sensory deficits. This is consistent with previous results where lesion volume on diffusion-weighted imaging has been shown to

Table 2
Association between white matter (ChaCo) and grey matter (NoDe) disruption scores with sensory deficit. The association between ChaCo and NoDe disruption scores of individual brain regions on acute imaging and sensory deficit (SSD; 193 minus RASP score) in the acute phase after stroke. Point estimates and standard errors (SE) for the effect of white and grey matter disruption on clinical outcome are extracted from the multiple linear regression models SSD ~ log(volume) + ChaCo and SSD ~ log(volume) + NoDe, respectively, and reported on the linear (rather than the response) scale. Adjusted P values are obtained from applying Holm's method (Sture Holm, 1979) to the unadjusted P values obtained from a *t*-test on the regression coefficients. The effect of the nuisance variable lesion volume is not reported.
(*) There was no stroke lesion with direct frontal pole involvement.

	ChaCo					NoDe				
	Estimate	SE	P	P_{adj}	AIC	Estimate	SE	P	P_{adj}	AIC
Supramarginal	2.47	0.61	1.10e-04	**0.005**	84.39	2.27	0.59	2.25e-04	**0.009**	84.92
Postcentral	2.55	0.68	3.18e-04	**0.013**	83.63	2.18	0.65	0.001	**0.041**	86.26
Transverse temporal	1.73	0.49	6.90e-04	**0.028**	83.65	1.58	0.45	5.99e-04	**0.024**	84.01
Precentral	2.95	0.93	0.002	0.076	86.87	2.26	1.04	0.032	1.000	90.50
Insula	1.84	0.60	0.003	0.102	87.63	1.52	0.52	0.004	0.164	87.68
Posterior cingulate	6.61	2.24	0.004	0.146	92.32	7.31	2.99	0.016	0.570	95.14
Superior temporal	1.53	0.61	0.013	0.469	87.97	1.49	0.58	0.012	0.443	88.94
Pars opercularis	1.35	0.54	0.015	0.515	88.81	1.24	0.50	0.015	0.557	89.83
Pars triangularis	1.37	0.58	0.020	0.670	90.35	1.30	0.56	0.021	0.719	92.26
Pars orbitalis	1.79	0.76	0.020	0.670	92.39	1.44	0.66	0.031	1.000	94.20
Lateral orbitofrontal	2.25	0.98	0.024	0.755	90.20	2.15	0.99	0.032	1.000	91.94
Frontal pole(*)	389.09	186.01	0.039	1.000	91.16	NA	NA			NA
Putamen	1.02	0.51	0.048	1.000	92.63	0.70	0.45	0.127	1.000	93.65
Pericalcarine	−6.53	3.34	0.053	1.000	97.25	−4.68	3.04	0.126	1.000	96.97
Rostral middle frontal	2.88	1.58	0.071	1.000	92.19	4.21	3.71	0.259	1.000	94.36
Fusiform	−5.98	3.29	0.072	1.000	96.01	−17.04	9.61	0.079	1.000	94.51
Paracentral	4.34	2.42	0.076	1.000	94.72	10.82	7.96	0.177	1.000	96.10
Thalamus	1.89	1.05	0.076	1.000	100.75	0.06	1.81	0.972	1.000	96.35
Lateral occipital	−2.87	1.61	0.078	1.000	94.26	−2.62	1.84	0.158	1.000	94.75
Hypothalamus	2.11	1.22	0.086	1.000	99.40	4.13	3.21	0.201	1.000	99.07
Medial orbitofrontal	6.56	3.79	0.087	1.000	93.37	8.04	5.20	0.125	1.000	95.15
Lingual	−8.29	4.80	0.087	1.000	96.93	−10.21	7.61	0.183	1.000	95.25
Caudate	0.95	0.55	0.090	1.000	93.84	0.32	0.53	0.553	1.000	95.37
Pallidum	0.83	0.48	0.090	1.000	93.63	0.79	0.51	0.129	1.000	93.67
Temporal pole	2.32	1.38	0.095	1.000	93.51	0.83	1.31	0.526	1.000	95.49
Banks STS	0.83	0.50	0.097	1.000	92.20	0.47	0.44	0.289	1.000	93.90
Superior frontal	7.24	4.56	0.115	1.000	92.12	4.99	41.48	0.905	1.000	95.99
Precuneus	−6.37	4.12	0.125	1.000	97.09	−22.90	19.85	0.251	1.000	63.46
Caudal middle frontal	1.42	0.92	0.126	1.000	93.13	0.56	1.41	0.691	1.000	95.65
Parahippocampal	−3.62	2.64	0.173	1.000	95.94	−20.15	99.83	0.840	1.000	10.99
Accumbens area	1.06	0.79	0.182	1.000	94.40	0.96	0.93	0.307	1.000	95.24
Hippocampus	−0.14	0.94	0.886	1.000	95.86	−1.49	1.13	0.191	1.000	96.04
Cuneus	−14.36	10.92	0.192	1.000	62.88	−9.26	9.90	0.352	1.000	90.22
Isthmus cingulate	−3.07	2.53	0.228	1.000	94.64	−10.41	10.29	0.314	1.000	96.13
Amygdala	0.78	0.75	0.300	1.000	93.89	0.45	0.60	0.452	1.000	95.06
Rostral anterior cingulate	2.81	2.77	0.314	1.000	94.62	1.60	12.86	0.901	1.000	96.03
Middle temporal	0.80	0.82	0.330	1.000	93.83	0.79	0.88	0.372	1.000	94.25
Caudal anterior cingulate	2.12	2.35	0.371	1.000	94.68	0.10	4.63	0.982	1.000	96.13
Inferior parietal	0.62	0.77	0.422	1.000	94.77	0.42	0.83	0.609	1.000	95.47
Superior parietal	−0.88	1.34	0.512	1.000	96.75	−1.50	1.89	0.429	1.000	97.19
Entorhinal	−1.70	2.28	0.456	1.000	96.18	2.17	3.07	0.482	1.000	95.70
Inferior temporal	−0.88	1.62	0.588	1.000	96.54	−1.79	3.17	0.573	1.000	96.47

be associated with severity of clinical symptoms and to explain approximately one third of the variance in the acute NIHSS score (Löuvbld et al., 1997). As a more specific neurological function, a reduced sensitivity to overall infarct size is expected for sensation.

When we quantified localised network disruption either a) geometrically by the relative overlap between lesion mask and grey matter parcel as a marker for direct ischaemic damage, or b) topologically by the proportion of incident fibre tracts running through the infarct site, the same set of cortical regions, consisting of postcentral, supramarginal, and transverse temporal gyri, showed a significant association with somatosensory deficits. Similar results with regards to the functional deficits associated with white and grey matter damage were previously reported from a functional MRI study, where no clinical difference in somatosensory performance were found in patients with either cortical or subcortical infarcts (Carey et al., 2011).

Brain areas identified by our lesion-network study are well known for somatosensory processing. The postcentral gyrus incorporates the primary somatosensory cortex comprising Brodman areas 1, 2, and 3a/b. It is the primary afferent cortical area for somatosensory stimulus inputs ascending from the thalamus (McGlone et al., 2002), has a medio-lateral and rostral-caudal somatotopic representation (Blankenburg, 2003) and is associated with sensory and even motor deficits if disrupted (Abela et al., 2012; Kessner et al., 2016). The supramarginal gyrus is part of the secondary and tertiary somatosensory cortex and plays thus a major role as associative somatosensory cortex – together with the parietal opercular cortex (Ruben et al., 2001). It is also thought to play a role in language recognition and empathy. Its location at the end of the Sylvian fissure in the border zone between temporal, parietal, and occipital lobe reflects its associative role. The transverse temporal gyrus is situated in close anatomical proximity to the parietal operculum and the supramarginal gyrus. The finding of its involvement in sensory deficits seems surprising, since the transverse temporal gyrus – Brodman area 41 or Heschl's gyrus respectively – is classically known as the primary auditory cortex in terms of its functional involvement. We interpret this result in two ways: firstly, the exact correspondence between cortical gyri, their segmentation in the Desikan-Killiany atlas, and their neurological function is not anatomically unique across individuals (Eickhoff et al., 2018), and our results suggest that at least part of the transverse temporal gyrus might directly contribute to sensory perception. Secondly, functional network studies suggest that somatosensory

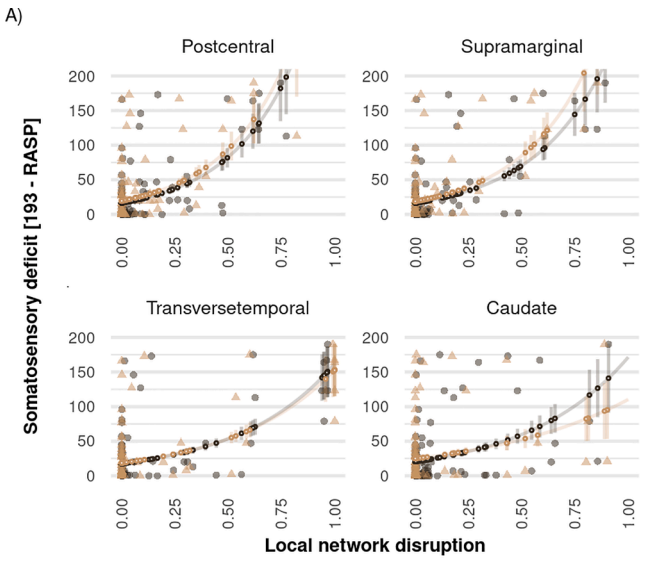

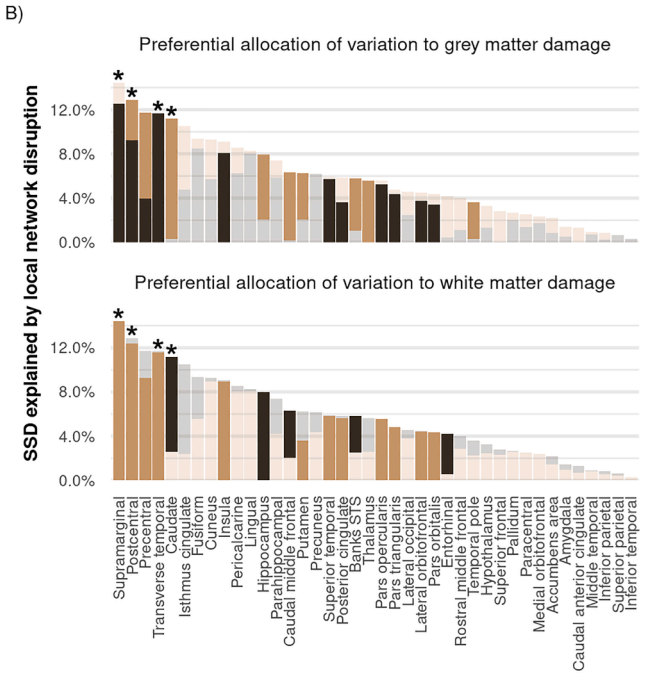

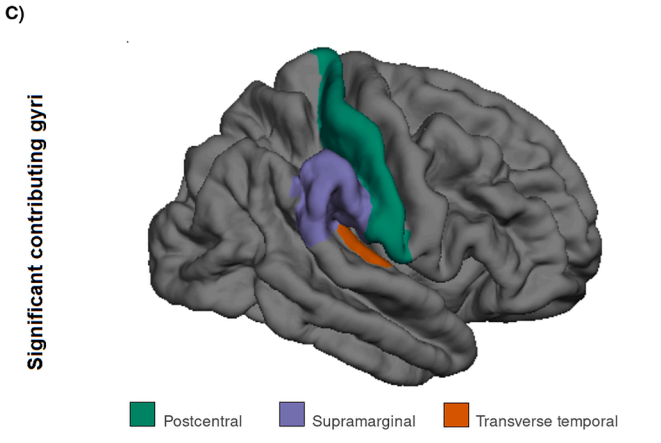

(caption on next column)

Fig. 4. Association between somatosensory system network disruption scores and sensory deficit. (A) Association between somatosensory system local network disruption scores and sensory deficit (193 minus RASP score) in the acute phase 3–5 days after stroke. Markers (ChaCo) and (NoDe) represent individual patient data; solid curves and conditional means in quasi-Poisson regression models; vertical line segments, pointwise 95% confidence intervals. (B) Amount of variation in sensory deficits explained by local network disruption beyond volume effect. After accounting for the effect of lesion volume, residual deviance was preferentially allocated to direct ischaemic damage of grey matter areas (top) or white matter tracts originating from those areas (bottom). Dark and light brown bars indicate significant contributions ($P < 0.05$, not corrected for multiple testing) to explained variation from either grey (■) or white (■) matter disruption. Non-significant ($P > 0.05$) individual contributions are greyed out. Regions in which the combined contribution of NoDe and ChaCo scores is statistically significant after correction for multiple testing (χ^2 test, Bonferroni-Holm) are marked (*). (C) Three-dimensional surface illustration of postcentral (elf green), supramarginal (chetwode blue), and transverse temporal (tawny) gyrus (Desikan-Killiany atlas) with significant associations between subcortical and cortical network disruptions and somatosensory deficits (Table 2). (For interpretation of the references to colour in this figure legend, the reader is referred to the web version of this article.)

perception involves complex interactions between a broad range of different cortical areas (De Bruyn et al., 2018; Goodin et al., 2018; Ingemanson et al., 2019). We speculate that, even if not involved in processing sensory inputs at an early stage, damage to the temporal gyrus might disrupt this network and impact on the higher cognitive aspects of perceiving sensory stimuli.

In this study, the location of and topologically specific connectivity disruptions induced by a stroke lesion were associated with somatosensory deficits even after controlling for the effect of infarct size and jointly explained up to 14% of additional variation in clinical deficits. Lesion volume has repeatedly been reported as an imperfect predictor for neurological deficit and functional outcome, with involvement of specific brain areas in the infarct more strongly associated with acute severity of symptoms (Payabvash et al., 2017) and residual disability (Cheng et al., 2014; Wu et al., 2015). In addition to both the micro- and macrostructural integrity of specific anatomical structures, such as the corona radiata or internal capsule (Lindenberg et al., 2010), the disruption of the brain's rich-club organization has recently been identified as an important topological determinant of functional outcome after stroke (Schirmer et al., 2019).

While both direct ischaemic damage and disconnection of somatosensory cortical areas are associated with clinical deficits, we found that the latter contains complementary information for the explanation of somatosensory deficits. Specifically, after adjusting for lesion volume and lesion overlap with somatosensory cortex, white matter damage could explain additional variation in behavioural outcome, while vice versa, damage to cortical brain regions had no additional predictive power after adjusting for white matter disruption. While interactions between grey matter and white matter damage have been described in stroke (Cheng et al., 2020), multiple sclerosis (Radetz et al., 2020), and vascular dementia (Jang et al., 2017), these findings on their differential relevance to explaining severity of somatosensory deficits are novel. Similarly, studies of the cerebral connectome using graph theory have hitherto concentrated on analysing the impact of damaged edges in a network only (van den Heuvel and Sporns, 2019). While information on cortical damage could, in principle, be incorporated into graph theoretical network analyses in the context of attributed graphs, applications to network neuroscience are yet to emerge.

With up to 3.6% excess clinical variation attributable to disconnection of somatosensory cortex alone (postcentral gyrus, lesion volume + NoDe + ChaCo vs lesion volume + NoDe, Fig. 4B), the absolute benefit of considering white matter disruption in addition to grey matter damage appears moderate. This is a reflection of the spatial distribution of ischaemic lesions in this cohort with a large number of infarcts with both cortical und subcortical components and only few purely cortical

infarcts (Table 1). Indeed, the observed strong correlation between markers of direct cortical damage (NoDe scores) and markers of disruption of incident fibre tracts (ChaCo scores) in almost all considered regions can be considered a consequence of the fact that white matter underlying a cortical region is likely to contain axons originating from or synapsing in that region. While the relevance of structural disconnection for somatosensory impairment in this cohort with mixed infarcts has been clearly demonstrated, it would be interesting to apply a similar analysis to patients with predominantly cortical or predominantly subcortical strokes, where an even larger synergy between the effects of disconnection and grey matter damage on clinical deficits would be expected.

Our results are constrained by a number of limitations. Firstly, the majority of patients in this sample has moderate to low severity of clinical deficits. Therefore, extrapolation to behaviour-brain damage association for severely affected patients is limited. Secondly, the spatial parcellation of the Desikan-Killiany parcellation did not afford the possibility differentiate between Brodman areas 3a/b, 1 and 2, which, collectively, form the primary somatosensory cortex. It also limited our ability to analyse and map the submodalities of somatosensory perception such as light touch, sharp-dull discrimination or proprioception. Previous results showing only subtle differences in the localisation of deficits in the somatosensory submodalities (Kessner et al., 2019) suggest that even a higher-resolution parcellation might not be sufficient and that a voxel-level analysis of the cortical connectivity map might be required to obtain robust results. The reliance on atlas data also limits the ability to account for inter-individual variability in somatotopic representations and functional connectivity changes during recovery that is known to occur at the sub-parcel level (Bannister et al., 2015). The resulting reduction in statistical power renders our analysis conservative, and false negatives with respect to subtle effects are therefore possible. The validity of the reported associations between network disruption and clinical deficits, however, is not affected by our reliance on atlas data. Third, in the present study, network disruption was quantified by projecting stroke lesions onto a set of reference tractograms. By the nature of this approach, only direct effects of the stroke lesion were taken into account, while clinical deficits resulting from cerebral hypoperfusion cannot be determined. Similarly, effects such as diaschisis or compensatory changes were not considered. Quantification of such effects, which we expect to be small in the acute phase, would require additional MRI sequences such as perfusion or diffusion tensor imaging (DTI) which were not obtained due to the clinical focus of the study. Until DTI becomes quicker, more robust to motion artefacts and thus more suitable for clinical population, indirect lesion network mapping provides a compromise of great utility between clinical practicability and anatomical precision (Salvalaggio et al., 2021, 2020, Umarova and Thomalla, 2020). We also note that the reference tractograms were obtained from young volunteers; however, possible biases arising from applying the NeMo tool to an elderly stroke population have previously been found not to interfere with meaningful clinical inferences (Kuceyeski et al., 2016, 2014, Schlemm et al., 2021). Imaging sequences from clinical routine with both MRI at 1.5 T and 3 T and, in two cases CT, were used. Due to the different spatial resolution of source images, the normalization processing might lead to small inaccuracies in some cases. Nevertheless, convincing results of the normalization (transformation and co-registration) were obtained and are shown in the Supplemental Fig. S5. Moreover, a sensitivity analysis confirmed that all presented results are robust with respect to excluding from the analysis the two patients who only received CT imaging (data not shown). Fourth, the decision to mirror all lesions to one hemisphere was made under the assumption of symmetry of the studied networks. This assumption is supported by structural and functional data in humans and animals which suggest that inter-individual variability occurs at the sub-parcel level and exceeds differences associated with laterality or handedness (Jung et al., 2003; Riddle and Purves, 1995; White et al., 1997). The alternative of computing lesion impact scores using hemisphere-naïve data and pooling left and right-sided lesions during statistical analysis would have represented an additional layer of complexity that, in the absence of a laterality-specific hypothesis, was avoided for the benefit of parsimony and ease of interpretation. Building on our results, it would be interesting to study, in the future, the effects of laterality and handedness on structural brain networks in stroke survivors with sensory deficits.

In conclusion, our results provide the first differential evaluation of grey and white matter disruption as structural correlates of acute somatosensory disturbance after ischaemic stroke. Our results underline that white matter integrity, in particular in a somatosensory network consisting of primary and secondary cortex, is an important prerequisite for normal processing of somatosensory inputs. We therefore propose that measures of structural disconnection, in conjunction with established markers of structural brain damage, might, in the future, inform targeted rehabilitation strategies to improve the long-term outcome of stroke survivors.

CRediT authorship contribution statement

Simon S. Kessner: Conceptualization, Methodology, Software, Formal analysis, Investigation, Writing - original draft, Visualization. **Eckhard Schlemm:** Conceptualization, Methodology, Software, Formal analysis, Writing - original draft, Visualization. **Christian Gerloff:** Validation, Resources, Writing - review & editing, Funding acquisition. **Götz Thomalla:** Conceptualization, Methodology, Validation, Resources, Writing - review & editing, Supervision, Project administration, Funding acquisition. **Bastian Cheng:** Conceptualization, Methodology, Software, Validation, Writing - review & editing, Supervision, Project administration, Funding acquisition.

Declaration of Competing Interest

The authors declare that they have no known competing financial interests or personal relationships that could have appeared to influence the work reported in this paper.

Acknowledgements

The authors wish to thank Ulrike Bingel for conceptional input for the study design and Alina Wesselovsky and Inka Homeyer for support with patient recruitment and study enrolment.

Funding

This research was supported by the German Research Foundation (DFG) SFB 936 “Multi-site Communication in the Brain” in project C2.

Appendix A. Supplementary data

Supplementary data to this article can be found online at https://doi.org/10.1016/j.nicl.2021.102698.

References

Abela, E., Missimer, J., Wiest, R., Federspiel, A., Hess, C., Sturzenegger, M., Weder, B., Valdes-Sosa, P.A., 2012. Lesions to primary sensory and posterior parietal cortices impair recovery from hand paresis after stroke. PLoS One 7 (2), e31275. https://doi.org/10.1371/journal.pone.0031275.

Baier, B., zu Eulenburg, P., Geber, C., Rohde, F., Rolke, R., Maihöfner, C., Birklein, F., Dieterich, M., 2014. Insula and sensory insular cortex and somatosensory control in patients with insular stroke. Eur. J. Pain 18 (10), 1385–1393. https://doi.org/10.1002/j.1532-2149.2014.501.x.

Bannister, L.C., Crewther, S.G., Gavrilescu, M., Carey, L.M., 2015. Improvement in touch sensation after stroke is associated with resting functional connectivity changes. Front. Neurol. 6, 1–15. https://doi.org/10.3389/fneur.2015.00165.

Blankenburg, F., 2003. Evidence for a rostral-to-caudal somatotopic organization in human primary somatosensory cortex with mirror-reversal in areas 3b and 1. Cereb. Cortex 13 (9), 987–993. https://doi.org/10.1093/cercor/13.9.987.

Boes, A.D., Prasad, S., Liu, H., Liu, Q.i., Pascual-Leone, A., Caviness, V.S., Fox, M.D., 2015. Network localization of neurological symptoms from focal brain lesions. Brain 138 (10), 3061–3075. https://doi.org/10.1093/brain/awv228.

Brodman, K., 1909. Vergleichende Lokalisationslehre der Grosshirnrinde. In ihren Principien dargestellt auf Grund des Zellenbaues. Johann Ambrosius Barth Verlag, Leipzig, Germany.

Carey, L.M., Abbott, D.F., Harvey, M.R., Puce, A., Seitz, R.J., Donnan, G. a, 2011. Relationship between touch impairment and brain activation after lesions of subcortical and cortical somatosensory regions. Neurorehabil. Neural Repair 25, 443–57. doi: 10.1177/1545968310395777.

Cheng, Bastian, Dietzmann, Philipp, Schulz, Robert, Boenstrup, Marlene, Krawinkel, Lutz, Fiehler, Jens, Gerloff, Christian, Thomalla, Götz, 2020. Cortical atrophy and transcallosal diaschisis following isolated subcortical stroke. J. Cereb. Blood Flow Metab. 40 (3), 611–621. https://doi.org/10.1177/0271678X19831583.

Cheng, Bastian, Forkert, Nils Daniel, Zavaglia, Melissa, Hilgetag, Claus C., Golsari, Amir, Siemonsen, Susanne, Fiehler, Jens, Pedraza, Salvador, Puig, Josep, Cho, Tae-Hee, Alawneh, Josef, Baron, Jean-Claude, Ostergaard, Leif, Gerloff, Christian, Thomalla, Götz, 2014. Influence of stroke infarct location on functional outcome measured by the modified rankin scale. Stroke 45 (6), 1695–1702. https://doi.org/10.1161/STROKEAHA.114.005152.

Cheng, B., Schlemm, E., Schulz, R., Boenstrup, M., Messé, A., Hilgetag, C., Gerloff, C., Thomalla, G., 2019. Altered topology of large-scale structural brain networks in chronic stroke. Brain Commun. 1 https://doi.org/10.1093/braincomms/fcz020.

Creutzfeldt, O.D., 1983. Cortex cerebri. Springer, Berlin.

De Bruyn, Nele, Meyer, Sarah, Kessner, Simon S., Essers, Bea, Cheng, Bastian, Thomalla, Götz, Peeters, Andre, Sunaert, Stefan, Duprez, Thierry, Thijs, Vincent, Feys, Hilde, Alaerts, Kaat, Verheyden, Geert, Hayasaka, Satoru, 2018. Functional network connectivity is altered in patients with upper limb somatosensory impairments in the acute phase post stroke: a cross-sectional study. PLoS One 13 (10), e0205693. https://doi.org/10.1371/journal.pone.0205693.

Desikan, Rahul S., Ségonne, Florent, Fischl, Bruce, Quinn, Brian T., Dickerson, Bradford C., Blacker, Deborah, Buckner, Randy L., Dale, Anders M., Maguire, R. Paul, Hyman, Bradley T., Albert, Marilyn S., Killiany, Ronald J., 2006. An automated labeling system for subdividing the human cerebral cortex on MRI scans into gyral based regions of interest. Neuroimage 31 (3), 968–980. https://doi.org/10.1016/j.neuroimage.2006.01.021.

Eickhoff, S.B., Amunts, K., Mohlberg, H., Zilles, K., 2006a. The human parietal operculum. II. Stereotaxic maps and correlation with functional imaging results. Cereb. Cortex 16, 268–279. https://doi.org/10.1093/cercor/bhi106.

Eickhoff, S.B., Schleicher, A., Zilles, K., Amunts, K., 2006b. The human parietal operculum. I. Cytoarchitectonic mapping of subdivisions. Cereb. Cortex 16, 254–267. https://doi.org/10.1093/cercor/bhi105.

Eickhoff, Simon B., Yeo, B.T. Thomas, Genon, Sarah, 2018. Imaging-based parcellations of the human brain. Nat. Rev. Neurosci. 19 (11), 672–686. https://doi.org/10.1038/s41583-018-0071-7.

Forkert, N.D., Cheng, B., Kemmling, A., Thomalla, G., Fiehler, J., 2014. ANTONIA perfusion and stroke: a software tool for the multi-purpose analysis of MR perfusion-weighted datasets and quantitative ischemic stroke assessment. Methods Inf. Med. 53 (06), 469–481. https://doi.org/10.3414/ME14-01-0007.

Fox, John, Weisberg, S., 2011. An R Companion to Applied Regression. Sage, Thousand Oaks CA.

Gleichgerrcht, E., Fridriksson, J., Rorden, C., Bonilha, L., 2017. Connectome-based lesion-symptom mapping (CLSM): a novel approach to map neurological function. NeuroImage Clin. 16, 461–467. https://doi.org/10.1016/j.nicl.2017.08.018.

Gleichgerrcht, E., Kocher, M., Nesland, T., Rorden, C., Fridriksson, J., Bonilha, L., 2015. Preservation of structural brain network hubs is associated with less severe post-stroke aphasia. Restor. Neurol. Neurosci. 34, 19–28. https://doi.org/10.3233/RNN-150511.

Goodin, P., Lamp, G., Vidyasagar, R., McArdle, D., Seitz, R.J., Carey, L.M., 2018. Altered functional connectivity differs in stroke survivors with impaired touch sensation following left and right hemisphere lesions. NeuroImage Clin. 18, 342–355. https://doi.org/10.1016/j.nicl.2018.02.012.

Grefkes, C., Fink, G.R., 2006. Somatosensorisches System, in: Funktionelle MRT in Psychiatrie Und Neurologie. Springer Berlin Heidelberg, Berlin, Heidelberg, pp. 279–296. doi:10.1007/978-3-540-68558-6_19.

Griffis, Joseph C., Metcalf, Nicholas V., Corbetta, Maurizio, Shulman, Gordon L., 2019. Structural disconnections explain brain network dysfunction after stroke. Cell Rep. 28 (10), 2527–2540.e9. https://doi.org/10.1016/j.celrep.2019.07.100.

Hawe, R.L., Findlater, S.E., Kenzie, J.M., Hill, M.D., Scott, S.H., Dukelow, S.P., 2018. Differential impact of acute lesions versus white matter hyperintensities on stroke recovery. J. Am. Heart Assoc. 7, 1–14. https://doi.org/10.1161/JAHA.118.009360.

Ingemanson, Morgan L., Rowe, Justin R., Chan, Vicky, Riley, Jeff, Wolbrecht, Eric T., Reinkensmeyer, David J., Cramer, Steven C., 2019. Neural correlates of passive position finger sense after stroke. Neurorehabil. Neural Repair 33 (9), 740–750. https://doi.org/10.1177/1545968319862556.

Jang, H., Kwon, H., Yang, J.J., Hong, J., Kim, Y., Kim, K.W., Lee, J.S., Jang, Y.K., Kim, S. T., Lee, K.H., Lee, J.H., Na, D.L., Seo, S.W., Kim, H.J., Lee, J.M., 2017. Correlations between gray matter and white matter degeneration in pure Alzheimer's disease, pure subcortical vascular dementia, and mixed dementia. Sci. Rep. 7, 1–9. https://doi.org/10.1038/s41598-017-10074-x.

Jung, Patrick, Baumgärtner, Ulf, Bauermann, Thomas, Magerl, Walter, Gawehn, Jochen, Stoeter, Peter, Treede, Rolf-Detlef, 2003. Asymmetry in the human primary somatosensory cortex and handedness. Neuroimage 19 (3), 913–923. https://doi.org/10.1016/S1053-8119(03)00164-2.

Kenzie, J.M., Semrau, J.A., Findlater, S.E., Yu, A.Y., Desai, J.A., Herter, T.M., Hill, M.D., Scott, S.H., Dukelow, S.P., 2016. Localization of impaired kinesthetic processing post-stroke. Front. Hum. Neurosci. 10, 1–13. https://doi.org/10.3389/fnhum.2016.00505.

Kessner, Simon S., Bingel, Ulrike, Thomalla, Götz, 2016. Somatosensory deficits after stroke: a scoping review. Top. Stroke Rehabil. 23 (2), 136–146. https://doi.org/10.1080/10749357.2015.1116822.

Kessner, Simon S., Schlemm, Eckhard, Cheng, Bastian, Bingel, Ulrike, Fiehler, Jens, Gerloff, Christian, Thomalla, Götz, 2019. Somatosensory deficits after ischemic stroke – time course and association with infarct location. Stroke 50 (5), 1116–1123. https://doi.org/10.1161/STROKEAHA.118.023750.

Kim, J S, 1992. Pure sensory stroke. Clinical-radiological correlates of 21 cases. Stroke 23 (7), 983–987. https://doi.org/10.1161/01.STR.23.7.983.

Klingner, C.M., Witte, O.W., Günther, A., 2012. Sensory syndromes. Front. Neurol. Neurosci. 30, 4–8. https://doi.org/10.1159/000333373.

Kuceyeski, Amy, Kamel, Hooman, Navi, Babak B., Raj, Ashish, Iadecola, Costantino, 2014. Predicting future brain tissue loss from white matter connectivity disruption in ischemic stroke. Stroke 45 (3), 717–722. https://doi.org/10.1161/STROKEAHA.113.003645.

Kuceyeski, Amy, Maruta, Jun, Relkin, Norman, Raj, Ashish, 2013. The Network Modification (NeMo) tool: elucidating the effect of white matter integrity changes on cortical and subcortical structural connectivity. Brain Connect. 3 (5), 451–463. https://doi.org/10.1089/brain.2013.0147.

Kuceyeski, Amy, Navi, Babak B., Kamel, Hooman, Raj, Ashish, Relkin, Norman, Toglia, Joan, Iadecola, Costantino, O'Dell, Michael, 2016. Structural connectome disruption at baseline predicts 6-months post-stroke outcome. Hum. Brain Mapp. 37 (7), 2587–2601. https://doi.org/10.1002/hbm.23198.

Kuceyeski, Amy, Navi, Babak B., Kamel, Hooman, Relkin, Norman, Villanueva, Mark, Raj, Ashish, Toglia, Joan, O'Dell, Michael, Iadecola, Costantino, 2015. Exploring the brain's structural connectome: a quantitative stroke lesion-dysfunction mapping study. Hum. Brain Mapp. 36 (6), 2147–2160. https://doi.org/10.1002/hbm.22761.

Lindenberg, R., Renga, V., Zhu, L.L., Betzler, F., Alsop, D., Schlaug, G., 2010. Structural integrity of corticospinal motor fibers predicts motor impairment in chronic stroke. Neurology 74 (4), 280–287. https://doi.org/10.1212/WNL.0b013e3181ccc6d9.

Löuvbld, Karl-Olof, Baird, Alison E., Schlaug, Gottfried, Benfield, Andrew, Siewert, Bettina, Voetsch, Barbara, Connor, Ann, Burzynski, Cara, Edelman, Robert R., Warach, Steven, 1997. Ischemic lesion volumes in acute stroke by diffusion-weighted magnetic resonance imaging correlate with clinical outcome. Ann. Neurol. 42 (2), 164–170. https://doi.org/10.1002/ana.410420206.

McGlone, Francis, Kelly, Edward F, Trulsson, Mats, Francis, Susan T, Westling, Göran, Bowtell, Richard, 2002. Functional neuroimaging studies of human somatosensory cortex. Behav. Brain Res. 135 (1-2), 147–158. https://doi.org/10.1016/S0166-4328(02)00144-4.

Meyer, S., Kessner, S.S., Cheng, B., Bönstrup, M., Schulz, R., Hummel, F.C., De Bruyn, N., Peeters, A., Van Pesch, V., Duprez, T., Sunaert, S., Schrooten, M., Feys, H., Gerloff, C., Thomalla, G., Thijs, V., Verheyden, G., 2016. Voxel-based lesion-symptom mapping of stroke lesions underlying somatosensory deficits. NeuroImage Clin. 10, 257–266. https://doi.org/10.1016/j.nicl.2015.12.005.

Page, Stephen J., Gauthier, Lynne V., White, Susan, 2013. Size doesn't matter: Cortical stroke lesion volume is not associated with upper extremity motor impairment and function in mild, chronic hemiparesis. Arch. Phys. Med. Rehabil. 94 (5), 817–821. https://doi.org/10.1016/j.apmr.2013.01.010.

Patel, Atul T., Duncan, Pamela W., Lai, Sue-Min, Studenski, Stephanie, 2000. The relation between impairments and functional outcomes poststroke. Arch. Phys. Med. Rehabil. 81 (10), 1357–1363. https://doi.org/10.1053/apmr.2000.9397.

Payabvash, S., Taleb, S., Benson, J.C., McKinney, A.M., 2017. Acute ischemic stroke infarct topology: association with lesion volume and severity of symptoms at admission and discharge. Am. J. Neuroradiol. 38 (1), 58–63. https://doi.org/10.3174/ajnr.A4970.

Preusser, S., Thiel, S.D., Rook, C., Roggenhofer, E., Kosatschek, A., Draganski, B., Blankenburg, F., Driver, J., Villringer, A., Pleger, B., 2014. The perception of touch and the ventral somatosensory pathway. Brain 138, 540–548. https://doi.org/10.1093/brain/awu370.

R Development Core Team 3.0.1., 2013. A Language and Environment for Statistical Computing, R Foundation for Statistical Computing. R Foundation for Statistical Computing, Vienna, Austria.

Radetz, Angela, Koirala, Nabin, Krämer, Julia, Johnen, Andreas, Fleischer, Vinzenz, Gonzalez-Escamilla, Gabriel, Cerina, Manuela, Muthuraman, Muthuraman, Meuth, Sven G., Groppa, Sergiu, 2020. Gray matter integrity predicts white matter network reorganization in multiple sclerosis. Hum. Brain Mapp. 41 (4), 917–927. https://doi.org/10.1002/hbm.v41.410.1002/hbm.24849.

Riddle, DR, Purves, D, 1995. Individual variation and lateral asymmetry of the rat primary somatosensory cortex. J. Neurosci. 15 (6), 4184–4195. https://doi.org/10.1523/JNEUROSCI.15-06-04184.1995.

Rorden, Chris, Karnath, Hans-Otto, Bonilha, Leonardo, 2007. Improving lesion-symptom mapping. J. Cogn. Neurosci. 19 (7), 1081–1088. https://doi.org/10.1162/jocn.2007.19.7.1081.

Rothwell, P., 2002. Stroke syndromes, 2nd Edn, and uncommon causes of stroke. Brain 125, 923–924. doi: 10.1093/brain/awf089.

Ruben, J., Schwiemann, J., Deuchert, M., Meyer, R., Krause, T., Curio, G., Villringer, K., Kurth, R., Villringer, A., 2001. Somatotopic organization of human secondary somatosensory cortex. Cereb. Cortex 11, 463–473. https://doi.org/10.1093/cercor/11.5.463.

Salvalaggio, A., De Filippo De Grazia, M., Zorzi, M., Thiebaut de Schotten, M., Corbetta, M., 2020. Post-stroke deficit prediction from lesion and indirect structural and functional disconnection. Brain 143, 2173–2188. doi:10.1093/brain/awaa156.

Salvalaggio, A., Pini, L., De Filippo De Grazia, M., Thiebaut De Schotten, M., Zorzi, M., Corbetta, M., 2021. Reply: Lesion network mapping: where do we go from here? Brain 144, e6–e6. doi: 10.1093/brain/awaa351.

Schirmer, M.D., Ktena, S.I., Nardin, M.J., Donahue, K.L., Giese, A.-K., Etherton, M.R., Wu, O., Rost, N.S., 2019. Rich-club organization: an important determinant of functional outcome after acute ischemic stroke. Front. Neurol. 10, 956. https://doi.org/10.3389/fneur.2019.00956.

Schlemm, E., Ingwersen, T., Königsberg, A., et al., 2021. Preserved structural connectivity mediates the clinical effect of thrombolysis in patients with anterior-circulation stroke. Nat. Commun. 12, 2590. https://doi.org/10.1038/s41467-021-22786-w.

Schlemm, E., Schulz, R., Bönstrup, M., Krawinkel, L., Fiehler, J., Gerloff, C., Thomalla, G., Cheng, B., 2020. Structural brain networks and functional motor outcome after stroke—a prospective cohort study. Brain Commun. 2 https://doi.org/10.1093/braincomms/fcaa001.

Shintani, S, Tsuruoka, S, Shiigai, T, 1994. Pure sensory stroke caused by a pontine infarct. Clinical, radiological, and physiological features in four patients. Stroke 25 (7), 1512–1515. https://doi.org/10.1161/01.STR.25.7.1512.

Sporns, O., 2013. The human connectome: origins and challenges. Neuroimage 80, 53–61. https://doi.org/10.1016/j.neuroimage.2013.03.023.

Holm, S., 1979. A simple sequentially rejective multiple test procedure. Scand. J. Stat. 6, 65–70.

Sullivan, Jane E., Hedman, Lois D., 2008. Sensory dysfunction following stroke: incidence, significance, examination, and intervention. Top. Stroke Rehabil. 15 (3), 200–217. https://doi.org/10.1310/tsr1503-200.

Umarova, R., Thomalla, G., 2020. Indirect connectome-based prediction of post-stroke deficits: prospects and limitations. Brain 143, 1966–1970. https://doi.org/10.1093/brain/awaa186.

Vaessen, M.J., Saj, A., Lovblad, K.-O., Gschwind, M., Vuilleumier, P., 2016. Structural white-matter connections mediating distinct behavioral components of spatial neglect in right brain-damaged patients. Cortex 77, 54–68. https://doi.org/10.1016/j.cortex.2015.12.008.

van den Heuvel, Martijn P., Sporns, Olaf, 2019. A cross-disorder connectome landscape of brain dysconnectivity. Nat. Rev. Neurosci. 20 (7), 435–446. https://doi.org/10.1038/s41583-019-0177-6.

White, L.E., Andrews, T.J., Hulette, C., Richards, A., Groelle, M., Paydarfar, J., Purves, D., 1997. Structure of the human sensorimotor system. II: Lateral symmetry. Cereb. Cortex 7, 31–47. https://doi.org/10.1093/cercor/7.1.31.

Winward, Charlotte E, Halligan, Peter W, Wade, Derick T, 2002. The Rivermead Assessment of Somatosensory Performance (RASP): standardization and reliability data. Clin. Rehabil. 16 (5), 523–533. https://doi.org/10.1191/0269215502cr522oa.

Wu, Ona, Cloonan, Lisa, Mocking, Steven J.T., Bouts, Mark J.R.J., Copen, William A., Cougo-Pinto, Pedro T., Fitzpatrick, Kaitlin, Kanakis, Allison, Schaefer, Pamela W., Rosand, Jonathan, Furie, Karen L., Rost, Natalia S., 2015. Role of acute lesion topography in initial ischemic stroke severity and long-term functional outcomes. Stroke 46 (9), 2438–2444. https://doi.org/10.1161/STROKEAHA.115.009643.

Zilles, K., Rehkämper, G., 1993. Funktionelle Neuroanatomie. Springer, Berlin.